

Article

Experimental and Numerical Studies of Sheet Metal Forming with Damage Using Gas Detonation Process

Sandeep P. Patil ^{1,*} , Kaushik G. Prajapati ¹, Vahid Jenkouk ¹, Herbert Olivier ²
and Bernd Markert ¹ 

¹ Institute of General Mechanics, RWTH Aachen University, Templergraben 64, 52062 Aachen, Germany; kaushik.prajapati@rwth-aachen.de (K.G.P.); jenkouk@iam.rwth-aachen.de (V.J.); markert@iam.rwth-aachen.de (B.M.)

² Shock Wave Laboratory, RWTH Aachen University, Schurzelter Str. 35, 52074 Aachen-Laurensberg, Germany; olivier@swl.rwth-aachen.de

* Correspondence: patil@iam.rwth-aachen.de; Tel.: +49-241-80-90036

Received: 9 November 2017; Accepted: 6 December 2017; Published: 10 December 2017

Abstract: Gas detonation forming is a high-speed forming method, which has the potential to form complex geometries, including sharp angles and undercuts, in a very short process time. Despite many efforts being made to develop detonation forming, many important aspects remain unclear and have not been studied experimentally, nor numerically in detail, e.g., the ability to produce sharp corners, the effect of peak load on deformation and damage location and its propagation in the workpiece. In the present work, DC04 steel cups were formed using gas detonation forming, and finite element method (FEM) simulations of the cup forming process were performed. The simulations on 3D computational models were carried out with explicit dynamic analysis using the Johnson–Cook material model. The results obtained in the simulations were in good agreement with the experimental observations, e.g., deformed shape and thickness distribution. Moreover, the proposed computational model was capable of predicting the damage initiation and evolution correctly, which was mainly due to the high-pressure magnitude or an initial offset of the workpiece in the experiments.

Keywords: gas detonation forming; finite element method; Johnson–Cook material model; damage

1. Introduction

Sheet metal forming basically consists of stretching and bending a thin sheet into the desired shape. The produced parts can be stiff and have good strength-to-weight ratios; therefore, these products are widely used for automobiles, domestic appliances, aircraft and food and drink cans. A large number of techniques is used to make sheet metal parts. In recent years, many aspects of sheet metal forming processes have been widely studied using electromagnetic forming, especially with regard to the behavior of materials under a high strain rate, the possible future applications and numerical modeling of the process, with several works dedicated to these topics [1–7]. Moreover, a detailed review of numerical simulations in sheet metal forming and potential developments is presented by Tekkaya [8].

DC04 steel has a good ductility level, which facilitates the production of complicated component shapes where required and even allowing deep pressing processes to be carried out. Here, cup formation of DC04 steel sheets was studied using the gas detonation forming technique. It is a highly dynamic manufacturing method, which involves the release of the stored energy in a very short interval of time. There are various high-speed forming processes, which are classified based on the type of energy transfer. This can be done by active media, accelerated mass or by active energy. Here, the high kinetic energy of a fluid medium is exploited, and it is used to collide the sheet-metal workpiece in the form of a shock front, which is produced as a result of the detonation of a mixture of gases like oxyhydrogen [9,10]. This forming process has many well-known advantages, namely

high degree of formability, capability to form complex geometries, including undercuts for high strain rate-dependent materials, and fine embossing without relief angle. The process consists of a clean combustion, having the advantages of easy automation and fewer safety regulations. The overall process and tooling costs are significantly reduced due to simplified tooling requirements compared to electromagnetic forming [11].

In previous works, Yasar and Yasar et al., conducted both experimental and numerical investigations of aluminum cup drawing using gas detonation. In the first work, 2D and 3D simulations were performed using both explicit and implicit dynamic analysis. The thickness and the final shape were compared to the experiments. Based on the term of deformed shape, the spring back predictions by explicit and implicit methods were discussed. In the second study, gas detonation forming experiments were performed using a mixture of acetylene and oxygen with an equal volume ratio. They also did the explicit dynamic simulations using ANSYS/LS-DYNA. The strain, thickness and volume of cup formation were compared [12,13]. Mokadem developed a dynamic forming limit diagram for this process [14]. Wijayathunga and Webb also developed a finite element model to simulate the experimental tests for the impulsive deep drawing of a brass square cup with the presence of a soft lead plug [15]. In the implementation of the finite element simulation, the effects of the medium impedance, wave reflection and refraction were considered to be negligible in order to improve the simplicity of the modeling procedure [15]. Mousavi et al., studied free underwater explosive forming of aluminum circular plates experimentally and analytically, using a central explosive charge on 2024 aluminum sheets [16]. In this study, numerical simulation results concluded that the friction coefficient and blank holder force must be sufficient and optimized in order to prevent uneven drawing and wrinkling [16].

Khalegi et al., worked on gas detonation forming of clamped circular mild steel with three conical dies having apex angles of 60° , 90° and 120° . They studied the influence of the initial ratio of the oxyhydrogen mixture and also the effect of three different initial pressures of 3, 4 and 5 bar. Moreover, FEM simulations were performed, and the results of thickness strain, hoop strain, thickness variation and deformed geometry were compared with the experiments [17]. Hashem Babaei et al., conducted experiments on clamped circular plates of mild steel, using impulse loading from the detonation of the oxygen and acetylene mixture at various volume ratios and different initial pressures. They developed an analytical and empirical model for their experiments to demonstrate the effect of the mechanical properties of the plate and gas, the impulse of applied load, plate geometry, the velocity of sound in different gases and the strain-rate sensitivity on the large deformation of circular plates in high rate energy forming [18,19]. Mirzababaie Mostofi et al., investigated the effect of the detonation of different oxyacetylene mixtures on the dynamic response of aluminum alloy and mild steel plates with different thicknesses. They examined the ductile transverse deformation of the clamped rectangular plates. Theoretical analysis was conducted, according to an upper bound solution and energy method, with theoretical models assuming a zero-order Bessel function of the first kind in the x and y directions for a transverse displacement profile to predict permanent deflections. To account for material strain rate sensitivity, a Cowper–Symonds model has been used and was compared to Jones' theoretical model [20]. In other works, they suggested new dimensionless numbers based on the dimensionless governing equations and using a new mathematical method, namely the singular value decomposition method. Their empirical model was validated against the experiments. The study revealed that the empirical model using the Cowper–Symonds constitutive equation predicted the ratio of midpoint deflection to the thickness more accurately than Jones' theoretical equation [21].

These studies are important to shed light on the gas detonation forming process. However, some of the important aspects of the experiments, as well as the simulations of sheet metal forming by this technique have not yet been studied in detail, e.g., the observation of sharp edges in the deformation process, the influence of the peak load, the reproduction of the sharp corners in the numerical analysis and, more importantly, damage. In the gas detonation forming process, fracture occurs in the sheet metal by ductile damage due to the development of micro-cracks associated with large straining or due to plastic instabilities associated with the sheet materials' micro-structure and boundary conditions.

Therefore, one of the main objectives of this work is to predict when and where the cracks can appear in the workpiece during the forming.

The present work investigates the gas detonation forming of DC04 steel cups. The 3D explicit dynamic finite element analyses are carried out using the LS-DYNA explicit solver [22]. The material description considered for this study is the Johnson–Cook plasticity material model. The deformed geometry of the cup and thickness distributions are compared with the experimentally-obtained values. The relative differences found between the experimental and simulation results are discussed. Finally, the fractured specimens in the experiments are studied using adapted damage parameters for the numerical simulations.

2. Methods and Setup

2.1. Experimental Setup

Figure 1 depicts the apparatus, and Figure 2 shows a schematic representation of the experimental setup of the gas detonation forming process. It consists of four major parts, i.e., detonation tube, die holder, die and sheet metal or workpiece. The detonation tube of 700 mm in length is clamped to the die holder, forming a tight seal between them. A small hole is drilled through both the die holder and die, which is connected to a vacuum pump. This is done to prevent the formation of an air cushion between the sheet metal and the die, enabling the sheet metal to perfectly sit into the die. Figure 3 shows the inner dimensions of the die. The diameter of the circular metal blank was 54 mm with a thickness of 1 mm. The inner diameter of the die was 30 mm. The detonation tube contains two piezo-electric sensors oriented coaxially and connected to the gas space by radial bores. The types of sensors used were Kistler 603B (closer to workpiece) and Kistler 601H.

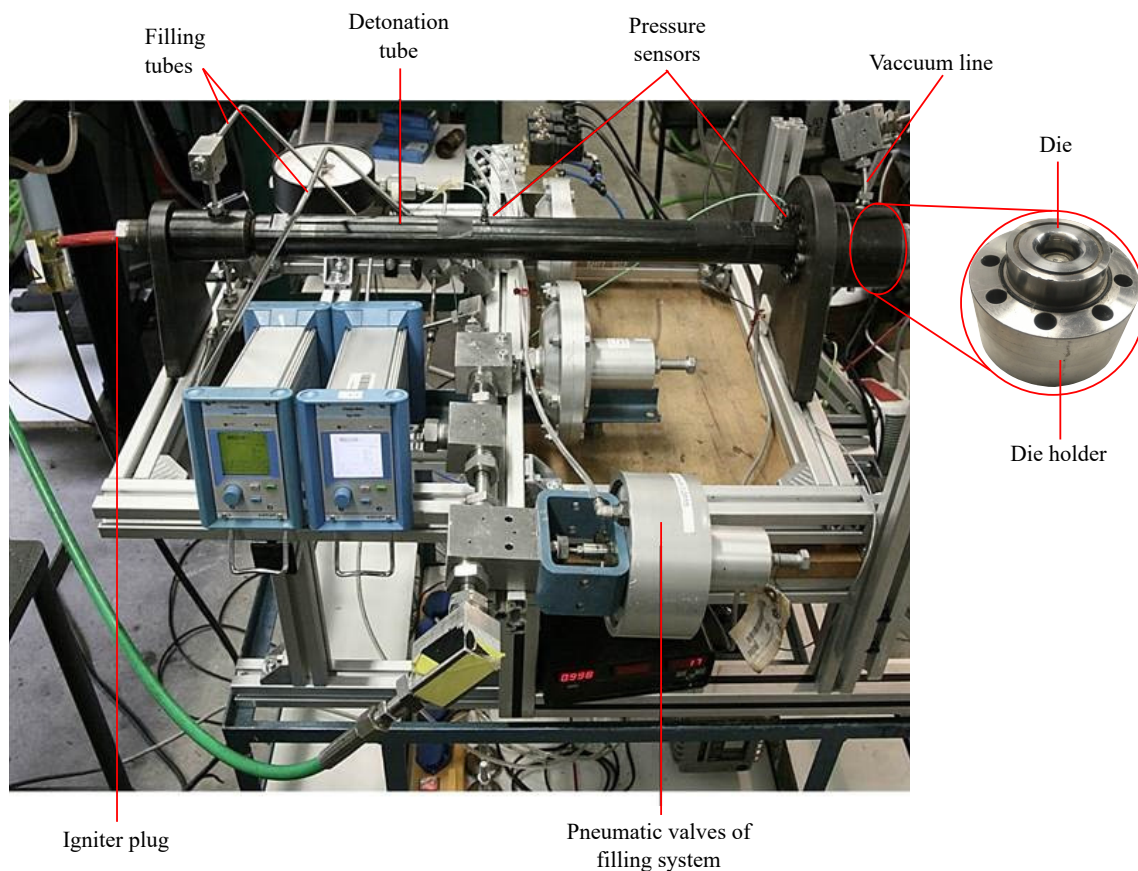


Figure 1. Gas detonation forming apparatus with peripheral equipment.

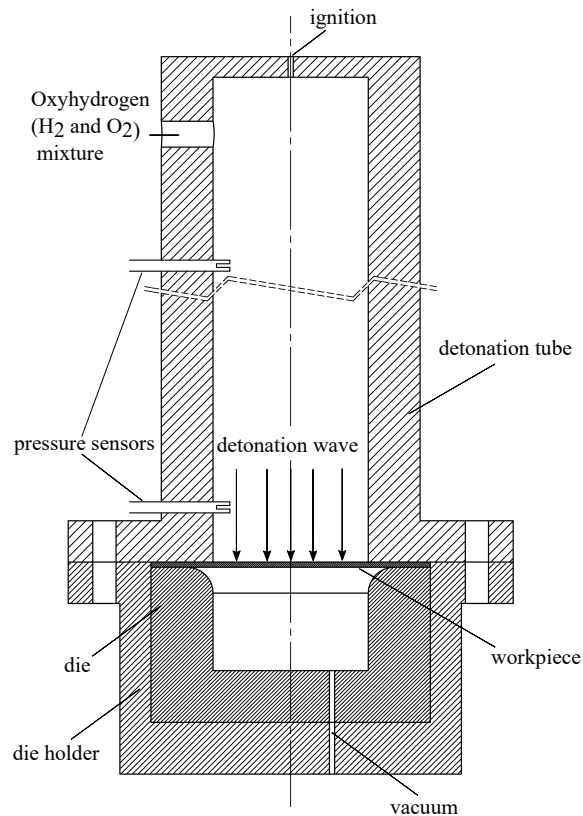


Figure 2. Schematic representation of the experimental setup of the gas detonation forming process.

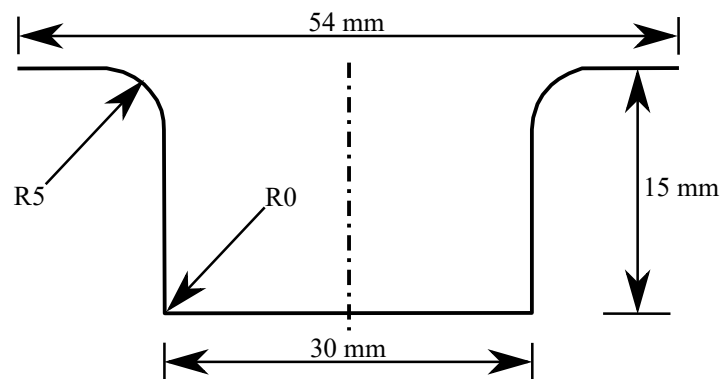


Figure 3. Internal dimensions of the die.

In the gas detonation process, the detonation tube is filled with oxyhydrogen. The gas mixture is compressed in the tube to the initial pressure. The mixture is ignited at the other end of the tube, causing the detonation wave to travel in the tube at constant supersonic velocity. A detonation wave is a joint complex of shock waves and reaction zones, implying shock waves that are strong enough to induce an immediate chemical reaction. The shock compression of the gas is sufficient to cause an instantaneous reaction of the oxyhydrogen mixture, which quickly leads to a chemical equilibrium. The released heat sustains the wave. The wave speed is approximately 3000 m/s; the thickness of wave is less than 1 mm; and the pressure directly behind it is about 20-times the initial pressure [23]. For this case study, the initial pressure in the tube was kept at 30 bar (3 MPa). The maximum pressure acting on the metal sheet was observed to be approximately 1500 bar (150 MPa). This maximum pressure loading, which occurs just at the beginning of the interaction of the detonation wave with the workpiece, is caused by the reflection of the detonation wave at the workpiece. This wave reflection is

so fast that during this very short interval of time, no or only a very small deformation of the metal sheet occurs [23]. For the prevention of overheating of the workpiece from hot detonated gas, moist filter paper was placed on the blank as thermal insulation.

The averaged pressure record of the sensor (close to the workpiece) is shown in Figure 4, which was obtained during the forming of DC04 specimens. The measured signals from the two sensors have been smoothed with a half-width of 10 μs to eliminate extreme oscillations. The second pressure rise is caused by the reflection at the end wall. The forming of the cup leads to a faster and further pressure drop following the detonation wave because of the increasing volume. All experiments were conducted at the Shock Wave Laboratory, RWTHAachen University.

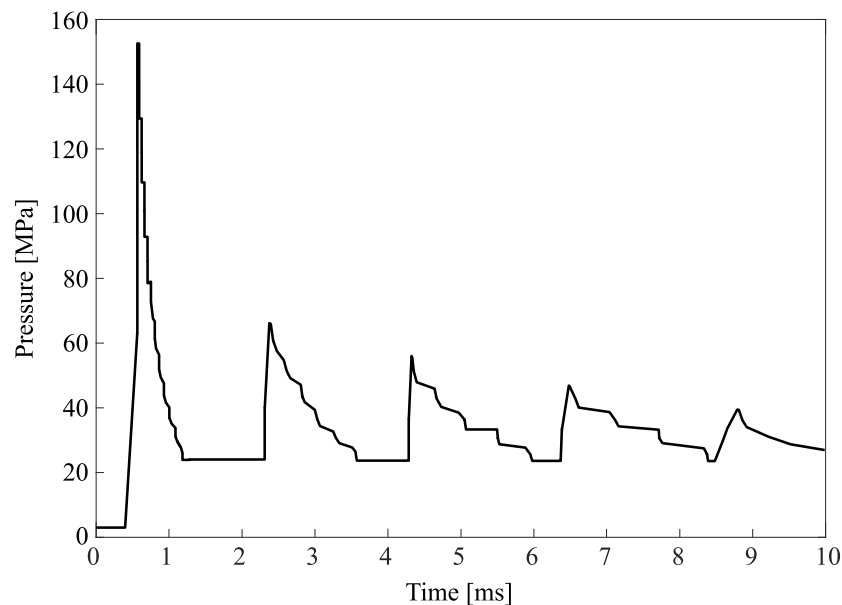


Figure 4. Averaged detonation pressure records from experiments.

2.2. Numerical Modeling

Gas detonation is a transient dynamic process involving shock waves transferring energy into the workpiece. The process simulation is based on the solution of dynamic equilibrium equations [24]. Hence, the simulations were done using an explicit time integration in the LS-DYNA solver (version: ls971 R7.1.1) [22]. Since we are interested in the deformation process of the workpiece and not in the shock wave propagation in the detonation tube, the problem was simplified by directly applying the detonation pressure as a load in the finite element (FE) models.

Figure 5 shows one-quarter section view of the 3D FE model. Due to the axial symmetry of the problem, only a quarter of the whole system with symmetric boundary conditions was considered to reduce the computational time. The model includes the die, the top plate (bottom part of the detonation tube) and the sheet metal workpiece. The one-quarter FE model was used to study the deformation of the workpiece into the cup with no misalignment. However, to study damage in the workpiece during forming, we considered the complete (full) model because the symmetry boundary conditions would highly influence the prediction of the damage areas. Moreover, offsets or improper alignment of the workpiece in experiments can be very well studied using the full model in order to capture workpiece formability in all directions.

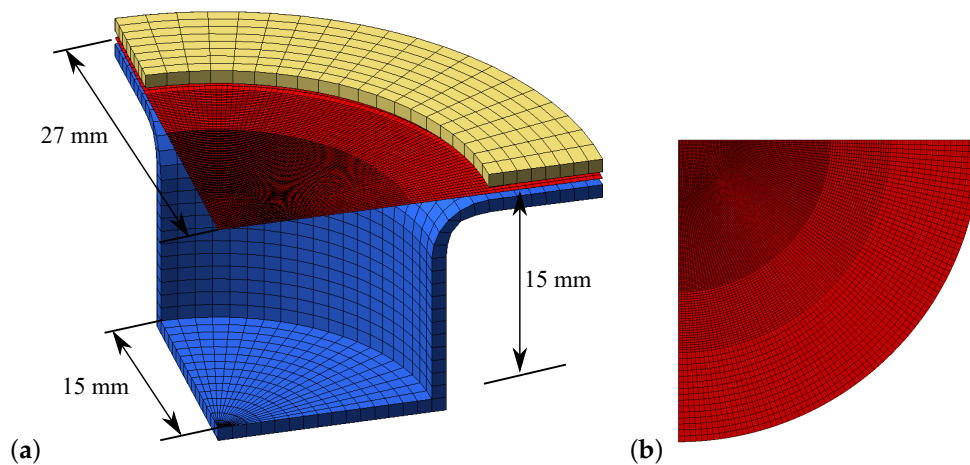


Figure 5. (a) One-quarter section view of the 3D finite element model; (b) FE meshed workpiece.

The die and the top plate were modeled using solid elements and rigid material (MAT_020), because of their high stiffness compared to the blank and as they are not the active components during the forming process. Belytschko–Tsay shell elements with five integration points [22] were used to create the meshed workpiece, which resulted in a total of 11,076 elements. The die and the holder were considered to be fixed, and the contact between them was defined using the surface-to-surface segment-based contact formulation [22], assuming planer segments. The pressure load was applied only on the free surface of the blank. According to the EN 10130-2006 standards, DC04 steel contains carbon, manganese, phosphorus and sulfur at 0.08% , 0.04% , 0.03% and 0.03% by weight, respectively. The mechanical properties of the blank DC04 are given in Table 1.

Table 1. Mechanical properties of DC04.

Property	Value
Young's modulus (GPa)	180
Poisson's ratio	0.3
Density (kg/m ³)	7870
Tensile strength (MPa)	210

The material model used for the workpiece was the Johnson–Cook phenomenological material model (MAT_015) [25], which is probably the most used and available in most of the commercial finite element commercial codes. This material model reproduces several important material responses observed in the forming, impact and penetration of metals. In this model, the three key plastic material responses are considered strain hardening, strain rate sensitivity and thermal softening. These three effects are combined in a multiplicative manner, such that the Johnson–Cook constitutive stress reads:

$$\sigma_y = \left(A + B\bar{\epsilon}^n \right) \left(1 + C \ln \frac{\dot{\epsilon}^p}{\dot{\epsilon}_0} \right) \left(1 - \left[\frac{T - T_{room}}{T_{melt} - T_{room}} \right]^m \right), \quad (1)$$

where $\bar{\epsilon}^p$ is the effective plastic strain, T_{room} the ambient temperature, T_{melt} the melting point or solidus temperature, T the effective temperature, A the yield stress, B the hardening modulus, n the strain exponent, m the temperature exponent and C the strain rate factor. Furthermore, $\dot{\epsilon}_0$ represents the strain rate for the quasi-static reference loading $\dot{\epsilon}_0 = 5.6 \times 10^{-4} \text{ s}^{-1}$ [26].

However, in this work, using the proposed strain rate by Verleysen et al. [26], we observed that there were no sharp corners at the bottom of the deformed cup; the final diameter of the cup did not match with the experimental value; and also, the formability for different loading profiles was not

similar to that of the experiments. All the above-mentioned numerical issues were due to the highly dynamic process. Schwer et al., introduced optional strain rate forms calibrated to laboratory data for A36 steel [27]. Comparing the calibrated model response to quasi-static A36 steel data, they illustrated the role of the $\dot{\epsilon}_0$ parameter in the Johnson–Cook material model. This is not simply a parameter for making the effective plastic strain-rate non-dimensional, as is often incorrectly cited, but this parameter must be specified as the effective plastic strain rate of the quasi-static testing. Therefore, in order to get the experimental shapes, the value of $\dot{\epsilon}_0$ was increased by two times, and the obtained results were close to the experimental ones. Hence, the different trial simulations were performed with increasing values of $\dot{\epsilon}_0$, and the results were compared with the experiments. Therefore, we propose a strain rate of $\dot{\epsilon}_0 = 7.3 \times 10^{-3} \text{ s}^{-1}$ for the gas detonation process.

The first bracketed term of the right-hand side of Equation (1) describes the isothermal static material behavior, i.e., the strain hardening of the yield stress. Consequently, the parameters A , B and n are determined using static tensile tests. The second term expresses the strain rate hardening with the parameter C . The last term represents a softening of the yield stress due to local thermal effects. In the experiments, a moistened filter paper was placed on the workpiece, in order to prevent the heating by contact with the hot detonated gas. Hence, the material surface remains unaffected despite the gas temperature. Therefore, in the Johnson–Cook material model, the thermal softening effect was not considered. The required material parameters for the simulations are given in Table 2 [26].

Table 2. Values for the Johnson–Cook material model parameters [26].

Property	Value
Yield stress, A (MPa)	162
Strength coefficient, B (MPa)	598
Deformation hardening, n	0.6
Strain rate coefficient, C	2.623
Deformation sensitivity, m	0.009

The ductile rupture of materials is described by three phases, namely void nucleation, growth and coalescence [28,29]. The void growth depends not only on the equivalent plastic strain, but also on triaxiality, which is defined as the ratio of the mean stress to the von Mises effective stress. Therefore, the damage behavior of a material depends strongly on the load type and on the geometry. In addition, the damage behavior is influenced by the strain rate.

To simulate the damage in the workpiece, damage parameters were included in the Johnson–Cook material model. Damage in the material tries to take path dependency into account by accruing the incremental effective plastic strain as the forming process proceeds [30]. In this material model, the failure strain is a function of the effective stress, the strain rate and the temperature. The equation of the fracture strain is given as:

$$\epsilon^f = [D_1 + D_2 \exp(D_3 \sigma^*)][1 + D_4 \ln \dot{\epsilon}^*][1 + D_5 T^*], \quad (2)$$

where D_1 to D_5 are five constants. σ^* is the ratio of pressure divided by effective stress:

$$\sigma^* = \frac{P}{\sigma_{eff}}. \quad (3)$$

where P is the average of the normal stresses and σ_{eff} is the von Mises equivalent stress. $\dot{\epsilon}^*$ is normalized effective plastic strain, given by:

$$\dot{\epsilon}^* = \frac{\dot{\epsilon}^p}{\dot{\epsilon}_0}. \quad (4)$$

and T^* is the homologous temperature:

$$T^* = \frac{T - T_{room}}{T_{melt} - T_{room}}. \quad (5)$$

The expression in the first set of brackets in Equation (2) represents that the strain to fracture decreases as the average normal stresses, P , increase. The second set of brackets represents the effect of the strain rate, and that in the third set of brackets represents the effect of temperature [30]. In this numerical simulation work, only D_1 to D_4 are considered, since we are assuming the temperature of the workpiece to be constant during the forming process.

The damage to an element is defined as:

$$D = \sum \frac{\Delta \bar{\epsilon}^p}{\epsilon^f} \quad (6)$$

where $\Delta \bar{\epsilon}^p$ is the increment of the equivalent plastic strain, which would occur during the integration cycle, and ϵ^f is the equivalent strain to fracture under the current condition of pressure, equivalent stress, strain rate and temperature. Fracture occurs when the damage parameter D reaches the value of one, and the corresponding failed elements are deleted.

3. Results and Discussion

3.1. Cup Formation

A number of gas detonation experiments of cup formation were carried out using a DC04 steel sheet of 1 mm in thickness and 54 mm in diameter. The shock wave acting on the blank was approximately 1500 bar (150 MPa). The blank sits perfectly into the die seat, with a depth of 15 mm. In our previous work [31], as well as Yasar [12], it is clear that when the applied load is triangular, i.e., load increases with a lower slope than that of the experiments, the spring-back effects are observed. In the present work, load was instantaneously (high slope of pressure loading profile) like that in the experiments, and hence, the spring-back effect was not observed. Since the process takes place in a very short period of time and at a very high-pressure, sharp corners were observed at the bottom of the cup. There were no observable wrinkles on the flange or on the skirt of the cup.

Figure 6 shows the qualitative comparison between the deformed shape of cups in the experiment and the numerical simulation. In the numerical simulations, the one-quarter section was considered with symmetry boundary conditions. The experimental pressure profile was the input loading curve for the simulations.



Figure 6. (a) Detonation formed cup in the shock tube; (b) Cup formation predicted by numerical simulations; (c) One-quarter section view of the FE model after the application of load.

Our numerical simulation studies produced remarkably similar results compared to the experiments. The numerical simulation shows no wrinkles on the flange or skirt of the formed cup (Figure 6). Furthermore, very sharp corners were observed at the bottom of the cup.

Figure 7 shows a comparison of the final diameters of the deformed cups in the experiment and simulation. The mean value of the final diameter of the workpiece was 44 mm, which was obtained

from eight samples in the experiment, and 44.6 mm was the diameter of the cup in the numerical simulation. In the experiments, it was unclear what caused the flange diameter to be 44 mm, i.e., friction or the inertia effects of the blank.

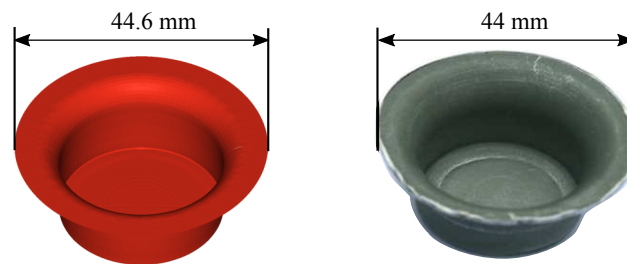


Figure 7. Diameter comparison of numerically- and experimentally-formed DC04 cups.

Therefore, different static and dynamic friction coefficients were considered between the workpiece and the top plate, as well as between the workpiece and the die. The detailed analysis is discussed in the Supplementary Materials. Initially, a static coefficient of friction of 0.6 and a dynamic coefficient of friction of 0.7 were considered between the workpiece and the top plate, as well as between the workpiece and die [32]. However, the outer diameter was nearly 53.9 mm, and also, the bottom corners were not sharp. In case the friction parameters were zeros, the outer diameter was nearly matched to the experimental diameter of 44.6 mm. Moreover, the bottom corners were sharp like the experimentally-formed cup. Therefore, we concluded that the final flange diameter is the result of the inertia effects.

Figure 8 depicts the shape of the deformed blank with respect to the loading time. The analysis of the blank shape with respect to the time highlights the fact that the whole deformation process takes place within the first approximately 60 μs , and the reflective waves do not play a major role in the formation of the cup.

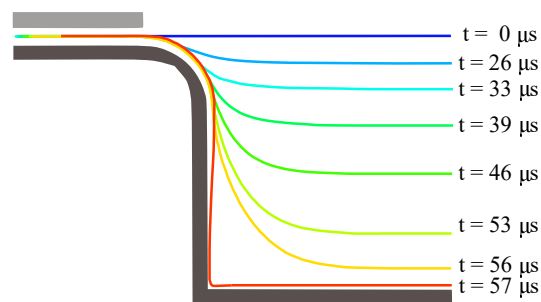


Figure 8. Cup shape formation during the simulation of the gas detonation forming process.

Figure 9 depicts the displacement of the center point of the blank over the time. From the graph, it is clear that the workpiece took some time initially to deform, and then, there is instantaneous deformation. There is no kink or decrease in the displacement of the center point of the workpiece; therefore, there was no spring back effect observed in the simulations.

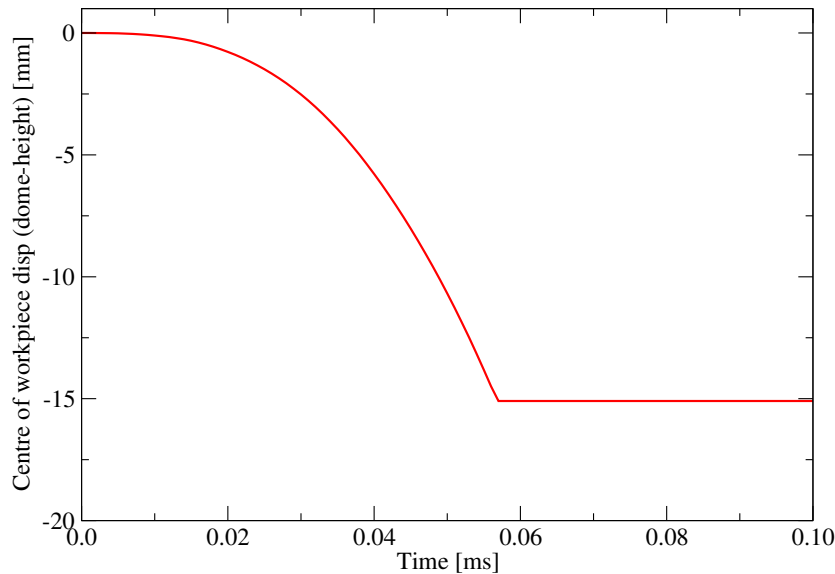


Figure 9. Displacement of the center point during cup formation in the simulations.

Thickness Variation

In our previous work [31,33], we concluded that the loading rate, i.e., the time instant at which the peak pressure acts on the blank, has a significant influence on the thickness distribution and the radial strain of the blank. The work highlighted the fact that the obtained results from the numerical model were very sensitive to the loading rate. Therefore, it is necessary to get an accurate experimental loading curve using well-calibrated measuring devices and to consider it in the numerical simulations.

The parameters of the Johnson–Cook material model can significantly affect the deformation behavior and the thickness distribution. One of the aims of this work was to correctly predict the thickness distribution in the numerical simulations along the base and the wall of the deformed cup. Figure 10 shows the thickness distribution along the initial radius of the workpiece. The obtained results from the numerical simulation were in good agreement with the experiments. The model was clearly able to predict a local minimum in the thickness value close to the 90° bend, which was towards the center of the cup (approximately 10 mm in radius). The minimum thickness obtained was nearly 0.6 mm. However, the area that stays between the die and top plate, which does not go into the cavity, experiences pure radial pulling. Moreover, due to the circumferential stresses, the thickness was increased [12,34].

In the literature, the thickness distribution has been studied using finite element models; however, experimental loading rates were not considered, and smooth variations of the thickness were observed [12,13]. In this work, an experimental loading rate was considered, and the simulations were competent to predict the experimental thickness variation pattern.

Along the wall of the cup, lower strain was observed suggesting preservation of wall thickness. On the outer area of the workpiece, a strain of approximately 0.1 was predicted due to material concentration, resulting in increased thickness. However, close to the center (approximately 5 mm radius), the radial strain was constant, where the thickness distribution was also nearly constant.

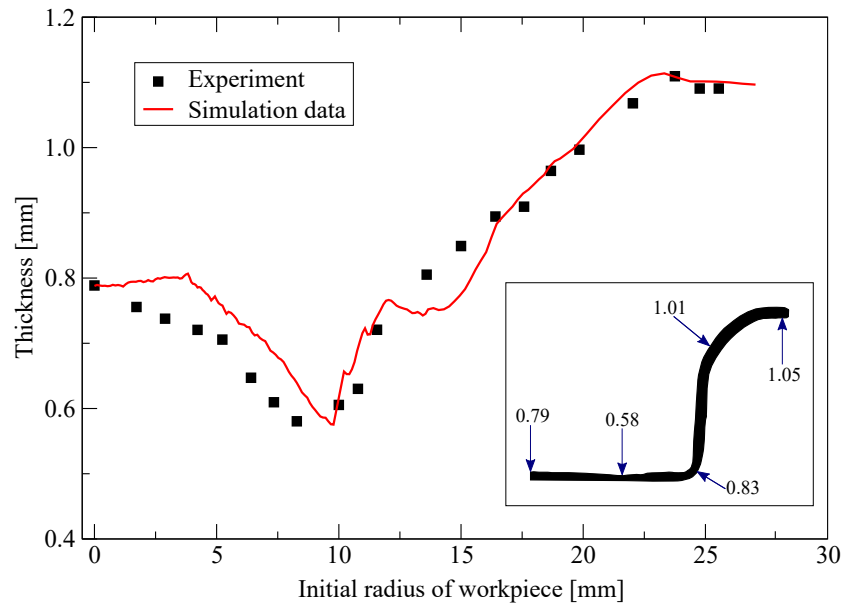


Figure 10. Thickness variation in the deformed cup with respect to the initial radius of the workpiece. Inset: half cut section view of the formed cup in the experiment (all the marked thickness values are in mm).

3.2. Damage in the Cup

Damage has a significant effect on the mechanical properties of a metal during deformation. The internal defects in the material act as nucleation sites and induce damage. The evolution of damage is essentially related to the dominant deformation mechanism. This mechanism depends on the deformation temperature, effective stress, strain rate, material micro-structure and chemical composition. In this work, the Johnson–Cook material model was considered; therefore, the focus was on the damage occurring in the forming process due to the effective stress and strain rate.

In 1985, the damage parameters of 4340 steel were investigated by Johnson and Cook [30]. Furthermore, the Johnson–Cook material model parameters were studied for Ti-6Al-4V and 7075-T6 aluminum alloy by Wang and Shi [35] and Zhang et al. [36], respectively. Recently, Buchkremer et al. [37] focused on the damage parameters of the Johnson–Cook material model of AISI 1045 steel. However, to the best of our knowledge, the damage parameters of DC04 steel have never been investigated for such a highly dynamic process. We have a number of fractured cups for different pressures, as well as misalignment of the workpiece from the experiments. The goal was to reproduce the experimental fracture patterns using the Johnson–Cook material model. Initially, the numerical simulations were performed using the proposed damage parameters of 4340 steel [30]. Then, we changed all the damage parameters in such way that the changed parameters can reproduce the experimental results. The damage parameters used in the Johnson–Cook material model are shown in Table 3.

Table 3. Damage parameters used in the Johnson–Cook material model.

Property	Value
D_1	0.02
D_2	3.9
D_3	−4.6
D_4	0.002

3.2.1. Pressure Magnitude

Figure 11 shows the variation in the pressure load curves acting on the blank to study its influence on the cup formation. As is clear from the Johnson–Cook damage material model, the fracture strain depends on the effective stress and strain rate. Therefore, in this work, the pressure load profile has been scaled, and we studied the resultant shape of the deformed cups with damage evolution.

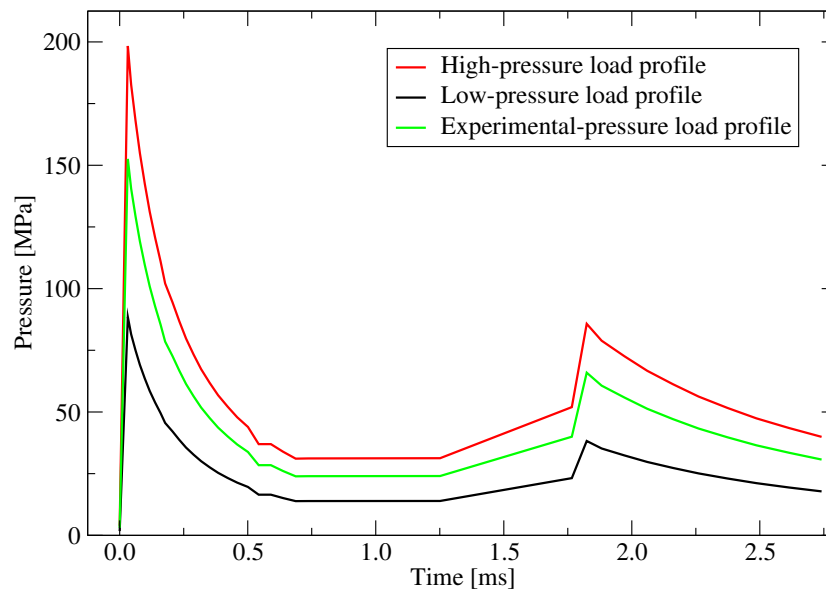


Figure 11. Pressure load curves acting on the workpiece in the experiments and simulations.

In the case of the low-pressure load profile, the workpiece was unable to deform completely. Figure 12 depicts the final shape of the workpiece when only 60% of the optimum experimental load, i.e., approximately 90 MPa peak pressure was applied. As mentioned earlier, the detonation process is highly inertia dependent, and low peak pressure was insufficient to introduce the required energy into the system. Hence, a dome-shaped output has been observed in the experiments, as well as the numerical simulations.



Figure 12. Comparison of the final shape obtained in the experiments (**top**) and numerical simulations (**bottom**) due to low-pressure load (60% of the optimum experimental load).

Figure 13 depicts the minor damage along the corner at the bottom. This kind of fracture was observed when pressure loading was increased up to 110% of the optimum experimental load. In the numerical simulations, a minor fracture was observed at the corners.



Figure 13. Damage occurring due to scaled load (110% of the optimum experimental load). Minor damage was observed along the corner. Comparison of the snapshots obtained in the numerical simulations (**top**) and experiments (**bottom**).

Figure 14 compares the simulation results at high pressure with those of the experiments. In the case of the high-pressure load, i.e., 130% of experimental optimum pressure load, the workpiece fails along the 90° bend; as a result, we observed a through hole in the workpiece. Similar observations were made in the simulations.



Figure 14. Damage caused by the high-pressure load profile (130% of experimental load). Snapshots of the fully damaged samples: numerical simulations (**left**) and experiments (**right**).

Figure 15 depicts the damage parameter distribution just before the fracture starts. In the vicinity of the bend, there was the highest stress concentration, as well as the maximum change in the effective

plastic strain observed. Ultimately, the highest (close to 1.0) value of the damage parameter D was observed in this region. Therefore, the cup failed along the corner at the bottom.

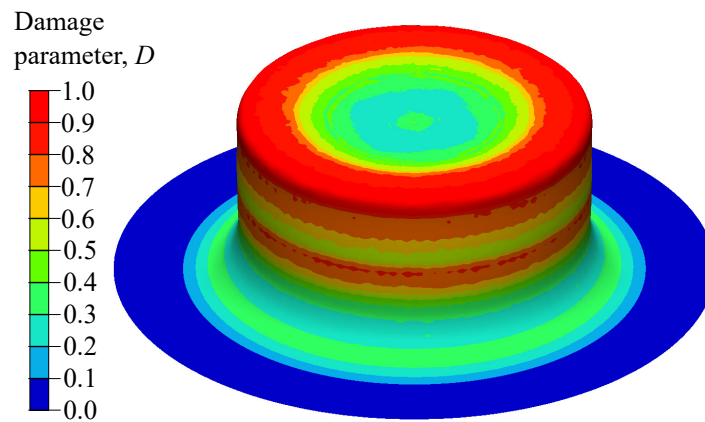


Figure 15. Distribution of damage parameter D in the high-pressure load profile simulation (the snapshot was taken just before $D = 1$).

3.2.2. Effect of Offset

A workpiece is properly placed between the die and the top plate, i.e., the center of the workpiece matches with the center of the die, as well as the top plate. This alignment is very important in order to apply the pressure load at the central part of the workpiece, and it deforms equivalently in all radial directions to form a perfect cup.

Offsetting of a workpiece, i.e., misalignment while placing of the workpiece in between the die and the top plate, can greatly affect the final shape. In this work, the offset influence on the final shape of the cup for the optimum experimental pressure load was investigated. For this purpose, we considered 3 mm of center offset of the workpiece in the experiments, as well as the numerical simulations. Figure 16 depicts the fracture occurring in the workpiece due to an initial misalignment of 3 mm between the blank and the die. A tearing effect was observed along the side where the material was less. This was because the amount of material available was less, and the strain value was high in this region. Subsequently, due to high energy in the process, the material failed along the skirt, as well as in the corners of the die, where the high local strain was concentrated.



Figure 16. Initial misalignment of 3 mm between the blank and the die. Fractured workpieces in numerical simulations (**top**) and specimen in the experiment (**bottom**).

Figure 17 shows the distribution of the damage parameter D in the simulation of a misaligned workpiece before damage. As previously mentioned, failure occurs when this parameter reaches 1.0. For the offset or misaligned workpiece simulation, it was observed that D increased rapidly in the region of high strain, where less material was available. Hence, the change in equivalent plastic strain was higher, implying that in Equation (6), the ratio would reach 1.0 more quickly, compared to the other regions. Therefore, failure occurred in this region.

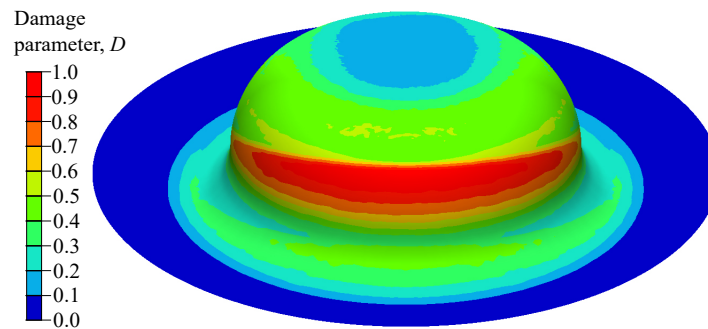


Figure 17. Distribution of damage parameter D in the simulation of the misaligned workpiece (the snapshot was taken just before the damage initiation; as the simulation continues, we obtained the final shape of the cup as shown in Figure 16).

4. Conclusions and Future Work

The experimental investigations of forming by gas detonation have shown the ability to produce sharp corners at the bottom of the formed DC04 steel cup without observable wrinkles on the flange or skirt. Furthermore, experiments conclude that the magnitude of the peak load has a high influence on the deformation.

Numerical simulations of the dynamic forming process were carried out with the Johnson–Cook plasticity model, which can mimic metal behavior on a wide range of strains, strain rates and temperatures. This plasticity model is the best choice to predict deformation during the forming process due to its moderate complexity and well-established methods to predict the material constants. Furthermore, damage parameters were included in this material model in order to study fracture behavior.

The proposed computational model was able to predict experimental results accurately, e.g., the shape of the cup and thickness distribution along the radius of the cup. Moreover, the model was capable of predicting damage initiation and evolution areas in the workpiece, which was mainly due to the high peak pressure magnitude and the initial misalignment of the same between the die and the top plate.

Further improvements can be made to the model by systematically performing a number of experiments of differently-shaped geometries. Furthermore, in the numerical study, temperature effects can be included and compared to the experiments. Moreover, the Johnson–Cook damage parameters can be studied in detail using more experiments and different sheet materials. This will help to approach more accurate results for a specific forming process.

Supplementary Materials: The supplementary materials are available online at www.mdpi.com/2075-4701/7/12/556/s1.

Acknowledgments: We thank Carlos Alberto Hernandez Padilla (Institute of General Mechanics, RWTH Aachen University) for fruitful discussions on the experimental data.

Author Contributions: Sandeep P. Patil and Bernd Markert proposed the idea; Sandeep P. Patil, Kaushik G. Prajapati and Bernd Markert conceived and designed the numerical simulations; Sandeep P. Patil, Kaushik G. Prajapati and Bernd Markert wrote the paper; Sandeep P. Patil, Kaushik G. Prajapati, Vahid Jenkouk and Herbert Olivier analyzed the data; Herbert Olivier performed the experiments.

Conflicts of Interest: The authors declare no conflict of interest.

References

1. Bruschi, S.; Altan, T.; Banabic, D.; Bariani, P.; Brosius, A.; Cao, J.; Ghiotti, A.; Khraisheh, M.; Merklein, M.; Tekkaya, A. Testing and modelling of material behaviour and formability in sheet metal forming. *CIRP Ann. Manuf. Techn.* **2014**, *63*, 727–749.
2. Marré, M.; Brosius, A.; Tekkaya, A. New aspects of joining by compression and expansion of tubular workpieces. *Int. J. Mater. Form.* **2008**, *1*, 1295–1298.
3. Marré, M.; Brosius, A.; Tekkaya, A.E. Joining by compression and expansion of (none-) reinforced profiles. *Adv. Mater. Res.* **2008**, *43*, 57–68.
4. Marré, M.; Ruhstorfer, M.; Tekkaya, A.; Zaeh, M. Manufacturing of lightweight frame structures by joining of (None-) reinforced profiles. *Adv. Mater. Res.* **2008**, *43*, 2573–2584.
5. Marré, M.; Ruhstorfer, M.; Tekkaya, A.; Zaeh, M. Manufacturing of lightweight frame structures by innovative joining by forming processes. *Int. J. Mater. Form.* **2009**, *2*, 307.
6. Martins, P.; Bay, N.; Tekkaya, A.; Atkins, A. Characterization of fracture loci in metal forming. *Int. J. Mech. Sci.* **2014**, *83*, 112–123.
7. Psyk, V.; Risch, D.; Kinsey, B.; Tekkaya, A.; Kleiner, M. Electromagnetic forming—A review. *J. Mater. Process. Technol.* **2011**, *211*, 787–829.
8. Tekkaya, A.E. State-of-the-art of simulation of sheet metal forming. *J. Mater. Process. Technol.* **2000**, *103*, 14–22.
9. Shchelkin, K.I.; Troshin, Y.K. *Gasdynamics of Combustion*, 1st ed.; Mono Book Corporation: Baltimore, MD, USA, 1965.
10. Honda, A.; Suzuki, M. Sheet metal forming by using gas imploding detonation. *J. Mater. Process. Technol.* **1999**, *85*, 198–203.
11. Mynors, D.J.; Zhang, B. Applications and capabilities of explosive forming. *J. Mater. Process. Technol.* **2002**, *125*, 1–25.
12. Yasar, M. Gas detonation forming process and modeling for efficient spring-back prediction. *J. Mater. Process. Technol.* **2004**, *150*, 270–279.
13. Yasar, M.; Demirci, H.I.; Kadi, I. Detonation forming of aluminium cylindrical cups experimental and theoretical modelling. *Mater. Design.* **2006**, *27*, 397–404.
14. El-Mokadem, A. Finite element modeling of sheet metal forming using shock tube. In Proceedings of the 9th International Conference Mechanical Design and Production (MDP-9), Cairo, Egypt, 8–10 January 2008.
15. Wijayathunga, V.; Webb, D. Experimental evaluation and finite element simulation of explosive forming of a square cup from a brass plate assisted by a lead plug. *J. Mater. Process. Technol.* **2006**, *172*, 139–145.
16. Mousavi, S.A.; Riahi, M.; Parast, A.H. Experimental and numerical analyses of explosive free forming. *J. Mater. Process. Technol.* **2007**, *187*, 512–516.
17. Khaleghi, M.; Aghazadeh, B.S.; Bisadi, H. Efficient oxyhydrogen mixture determination in gas Detonation forming. *Int. J. Mech. Mechatron. Eng.* **2013**, *7*, 1748–1754.
18. Babaei, H.; Mostofi, T.M.; Sadraei, S.H. Effect of gas detonation on response of circular plate-experimental and theoretical. *Struct. Eng. Mech.* **2015**, *56*, 535–548.
19. Babaei, H.; Mostofi, T.M.; Alitavoli, M.; Darvizeh, A. Empirical modelling for prediction of large deformation of clamped circular plates in gas detonation forming process. *Exp. Technol.* **2016**, *40*, 1485–1494.
20. Mirzababaie Mostofi, T.; Babaei, H.; Alitavoli, M. Experimental and theoretical study on large ductile transverse deformations of rectangular plates subjected to shock load due to gas mixture detonation. *Strain* **2017**, doi:10.1111/str.12235.
21. Mostofi, T.M.; Babaei, H.; Alitavoli, M. The influence of gas mixture detonation loads on large plastic deformation of thin quadrangular plates: Experimental investigation and empirical modelling. *Thin-Walled Struct.* **2017**, *118*, 1–11.
22. *LS-DYNA Theory Manual*; Livermore Software Technology Corporation: Livermore, CA, USA, 2006.
23. Kleiner, M.; Hermes, M.; Weber, M.; Olivier, H.; Gershteyn, G.; Bach, F.W.; Brosius, A. Tube expansion by gas detonation. *Prod. Eng.* **2007**, *1*, 9–17.
24. Nikiforakis, N.; Clarke, J. Numerical studies of the evolution of detonations. *Math. Comput. Model.* **1996**, *24*, 149–164.

25. Johnson, G.R.; Cook, W.H. A constitutive model and data for metals subjected to large strains, high strain rates and high temperatures. In Proceedings of the 7th International Symposium on Ballistics, The Hague, The Netherlands, 19–21 April 1983; Volume 21, pp. 541–547.
26. Verleysen, P.; Peirs, J.; Van Slycken, J.; Faes, K.; Duchene, L. Effect of strain rate on the forming behaviour of sheet metals. *J. Mater. Process. Technol.* **2011**, *211*, 1457–1464.
27. Schwer, L. Optional strain-rate forms for the Johnson Cook constitutive model and the role of the parameter Epsilon_0. In Proceedings of the 6th European LS-DYNA Users' Conference, Frankenthal, Germany, October 2007; pp. 11–22.
28. Schmitt, J.; Jalinier, J. Damage in sheet metal forming—I. Physical behavior. *Acta Mater.* **1982**, *30*, 1789–1798.
29. Jalinier, J.; Schmitt, J. Damage in sheet metal forming—II. Plastic instability. *Acta Mater.* **1982**, *30*, 1799–1809.
30. Johnson, G.R.; Cook, W.H. Fracture characteristics of three metals subjected to various strains, strain rates, temperatures and pressures. *Eng. Fract. Mech.* **1985**, *21*, 31–48.
31. Patil, S.P.; Popli, M.; Jenkouk, V.; Markert, B. Numerical modelling of the gas detonation process of sheet metal forming. *J. Phys. Conf. Ser.* **2016**, *734*, 032099.
32. Sullivan, J.F. *Technical Physics*, 99th ed.; Wiley: Hoboken, NJ, USA, 1988.
33. Jenkouk, V.; Patil, S.; Markert, B. Joining of tubes by gas detonation forming. *J. Phys. Conf. Ser.* **2016**, *734*, 032101.
34. Hosford, W.F.; Caddell, R.M. *Metal Forming: Mechanics and Metallurgy*; Cambridge University Press: Cambridge, UK, 2011.
35. Wang, X.; Shi, J. Validation of Johnson-Cook plasticity and damage model using impact experiment. *Int. J. Impact Eng.* **2013**, *60*, 67–75.
36. Zhang, D.N.; Shangquan, Q.Q.; Xie, C.J.; Liu, F. A modified Johnson–Cook model of dynamic tensile behaviors for 7075-T6 aluminum alloy. *J. Alloys Compd.* **2015**, *619*, 186–194.
37. Buchkremer, S.; Wu, B.; Lung, D.; Münstermann, S.; Klocke, F.; Bleck, W. FE-simulation of machining processes with a new material model. *J. Mater. Process. Technol.* **2014**, *214*, 599–611.



© 2017 by the authors. Licensee MDPI, Basel, Switzerland. This article is an open access article distributed under the terms and conditions of the Creative Commons Attribution (CC BY) license (<http://creativecommons.org/licenses/by/4.0/>).